

LA-UR-23-21746

Approved for public release; distribution is unlimited.

Title: A Prototype Thick-Target Bremsstrahlung Model with Angularly-Dependent Emission in the MCNP6 Code

Author(s): Bolding, Simon R.
Giron, Jesse Frank

Intended for: Report

Issued: 2023-02-21



Los Alamos National Laboratory, an affirmative action/equal opportunity employer, is operated by Triad National Security, LLC for the National Nuclear Security Administration of U.S. Department of Energy under contract 89233218CNA000001. By approving this article, the publisher recognizes that the U.S. Government retains nonexclusive, royalty-free license to publish or reproduce the published form of this contribution, or to allow others to do so, for U.S. Government purposes. Los Alamos National Laboratory requests that the publisher identify this article as work performed under the auspices of the U.S. Department of Energy. Los Alamos National Laboratory strongly supports academic freedom and a researcher's right to publish; as an institution, however, the Laboratory does not endorse the viewpoint of a publication or guarantee its technical correctness.

A Prototype Thick-Target Bremsstrahlung Model with Angularly-Dependent Emission in the MCNP6[®] Code

Simon R. Bolding and Jesse F. Giron

1 Summary

This document summarizes the current thick-target bremsstrahlung (TTB) model in MCNP and provides test results for an alternative implementation to improve the accuracy with reduced cost compared to full electron transport. It has been observed that the current TTB model produces inaccurate results in problems where the medium is thick with respect to electrons, but the photon distribution in the problem has a strong directionality. An example of such a simulation is detectors surrounding a metal target irradiated with a radiographic beam of high energy photons. The primary cause of this discrepancy is the current TTB method emits all bremsstrahlung photons in the same direction as the primary electron produced from each (γ, e^\pm) interaction, leading to artificially forward peaked photon distributions for intermediate to high-energy incident photons.

To improve the TTB model, we have implemented an angularly-dependent TTB model in a developer version of the MCNP6^{®1} code; for developers, this was done on the branch `prototype/angular_ttb` in the `mcnp6` repo on bitbucket. The angularly-dependent TTB model accounts for the energy and scattering of electrons as they slow down in the current material, but does not sample the computationally expensive energy straggling, secondary electron events, and tracking electrons; this approach is significantly less computationally expensive than full electron transport and can be comparable to the original TTB method for problems with sufficiently complex materials and geometry. To evaluate the method, we have modeled a simple problem of a beam of 5 MeV photons incident on a sphere of plutonium surrounded by detectors at different deflection angles. For this problem, the angularly-dependent TTB produces a photon flux within 8.0% for a 90 degree deflection angle and 0.8% along the beam axis, as compared to the electron transport solution. This is an improvement compared to a 43% and 81% discrepancy with the original TTB method, respectively.

The rest of this work includes the following: the first section details the current TTB treatment in MCNP, which has not been well documented elsewhere. Then, the modified TTB algorithm is detailed and the approximations compared to the condensed history algorithm are compared. Results are given comparing the two TTB methods to the condensed history transport algorithm. The appendix includes details for code developers on relevant electron transport implementation details and potential code improvements for future work.

¹MCNP6[®] and Monte Carlo N-Particle[®] are registered trademarks owned by Triad National Security, LLC, manager and operator of Los Alamos National Laboratory. Any third party use of such registered marks should be properly attributed to Triad National Security, LLC, including the use of the ® designation as appropriate. Any questions regarding licensing, proper use, and/or proper attribution of Triad National Security, LLC marks should be directed to trademarks@lanl.gov. The trademark logo will not be explicitly used for the remainder of this document.

2 Original Treatment of Thick-Target Bremsstrahlung (TTB) in the MCNP Code

The details of the implementation of the TTB model is not well-documented in the MCNP manual or other available references. Thus, we will summarize the implementation of the current TTB model in MCNP for completeness.

The TTB implementation uses the same electron cross sections and production data as the condensed history algorithm. Details on the condensed history algorithm are described in Ref. [1]. The relevant detail for TTB is that the condensed history algorithm has data formulated with a continuous slowing down approximation (CSDA) with energy-dependent properties evaluated at points on a fixed energy grid. Electron properties for an electron in energy group g are linearly interpolated between the group boundaries E_g and E_{g+1} . There are G total groups, ordered by descending energy, with the final end-point energy based on the electron energy cutoff.

The TTB model samples photons from approximate distributions based on the expected emission if the initial electron were to slow to the energy cutoff, in the current material. When the electron is converted to photons using the TTB model, the total number of photons to be produced is sampled, and the energy of each emitted photon is sampled independently. The emitted bremsstrahlung photons are defined to be traveling in the same direction as the incident electron, which is a poor assumption for photons emitted towards the end of the range of an initially energetic electron. The photons are emitted at the location that the electron was created. In the MCNPv6.3 code, sampling of TTB photons is implemented in the `ttbr.F90` file.

2.1 Sampling the Number of Bremsstrahlung Photons

Given an electron with kinetic energy E_e , in group g with bounds E_{g+1} and E_g , the number of bremsstrahlung photons emitted $N_{\text{brem}}(E_e)$ is calculated as the expected photon emission rate if the electron were to slow to rest in it's current material. In terms of the continuous slowing down approximation, for an electron slowing along a path s , this is defined as the integral

$$N_{\text{brem}}(E_e) = \int_{E_{\text{cut}}}^{E_e} \frac{\sigma_{\text{brem}}(E_e)}{S(E)} dE = \int_{R(E_{\text{cut}})}^{R(E_e)} \sigma_{\text{brem}}(E') ds(E') \quad (1)$$

where $\sigma_{\text{brem}}(E)$ is the *microscopic* differential cross section for bremsstrahlung radiative energy loss, E_{cut} is some cutoff energy required because of divergence of the continuous cross section at zero energy, and R and S are the total range and stopping power of an electron as a function of energy. In the MCNP code, the cutoff energy is based on the photon cutoff energy because the TTB model is used when the electron cutoff energy is higher than the photon cutoff energy. It is noted that the range here has units of atoms per barn, as it includes a multiplication by the material atom density. The stopping power includes a division by the material atom density.

Using the condensed history data tabulated on an energy grid, the value of $N_{\text{brem}}(E)$ is calculated at each energy grid point using a midpoint quadrature as

$$N_{\text{brem},g} = \sum_{g'=g}^G \frac{1}{2} (\sigma_{\text{brem},g'} + \sigma_{\text{brem},g'+1}) (R_{t,g'} - R_{t,g'+1}). \quad (2)$$

Here, $R_{t,g}$ is the total range (collisional plus radiative) of the electron (in atoms per barn), $\sigma_{\text{brem},g'}$ is the bremsstrahlung cross section evaluated at the group edge energies (in barn per atom), and both

are for the material of the cell the electron was created in. The above equation can also be viewed intuitively from a traditional Monte Carlo perspective. Over a small path length, the difference in ranges gives the distance that an electron will travel upon entering the group at energy E_g , and the linearly averaged bremsstrahlung cross-section gives the expected amount of bremsstrahlung photons produced per unit path-length traveled across the group. During transport, for an electron with energy E_e , the value of $N_{\text{brem},e}$ is computed with linear interpolation based on the fractional location of E_e between the group bounds f as

$$N_{\text{brem},e} = (1 - f)N_{\text{brem},g} + fN_{\text{brem},g+1}. \quad (3)$$

The number of photons actually produce is then sampled to the nearest integer as $N_{\text{brem}} = \lfloor \eta + N_{\text{brem},e} \rfloor$ where η is a uniform random number.

2.2 Sampling the Energy of Bremsstrahlung Photons

Once the number of photons is selected, the energy of the emitted photons are sampled independently using the appropriate bremsstrahlung emission energy distribution averaged over the electron slowing down. MCNP uses data from the ITS tables in the el03 database, formatted as ACE files, to load in tabulated data. The tabulated data provides the differential cross section (DCS) for the radiative loss to bremsstrahlung photon as a function of the photon energy and electron energy. This data is tabulated as a “scaled” DCS, which is a function of the dimensionless quantity κ defined as the ratio of the photon emission energy to the energy of the electron at the point of emission. The original reference for this data is given in the MCNP manual, but Ref. [2] gives more detail on the interpretation and justification for this data and its formulation.

In the file `xsgen.F90` of MCNP, the bremsstrahlung radiative loss DCS is loaded from the files and adjusted to include correction terms. The DCS is then integrated and normalized to form a cumulative probability density function (CDF) $F(\kappa, E_g)$ for κ , based on a piece-wise linear PDF in κ , at each electron energy point. For bremsstrahlung events in the regular condensed-history algorithm, a value of κ is sampled using this CDF, quadratically interpolated between electron energy points, and multiplied by the electron energy to produce the appropriate energy of the emitted photon. For the TTB algorithm, the distribution needs to be averaged over the slowing down of the electrons, weighted by production cross sections. The unnormalized, averaged cumulative distribution for κ given a bremsstrahlung photon was produced from an electron that slowed to rest from an initial energy E_g is computed as

$$\begin{aligned} \bar{F}(\kappa_j, E_g) = & \sum_{E_{g'} > \kappa_j E_g} \frac{1}{2} F\left(\kappa_j \frac{E_g}{E_{g'}}, E_{g'}\right) (\sigma_{\text{brem},g'} + \sigma_{\text{brem},g'+1}) (R_{t,g'} - R_{t,g'+1}) + \\ & \sum_{E_{g'} < \kappa_j E_g} \frac{1}{2} 1 (\sigma_{\text{brem},g'} + \sigma_{\text{brem},g'+1}) (R_{t,g'} - R_{t,g'+1}), \quad (4) \end{aligned}$$

where κ_j is stored on a fixed grid independent of material and number of groups, defined by the original data. The above tabular CDF is then re-normalized such that the integral over all κ is 1 for each E_g . The splitting into two summations accounts for the fact that for a given value E_g , a sampled value of κ yields a photon of energy $E_g \kappa$. If $E_g \kappa$ is greater than $E_{g'}$, where $E_{g'}$ represents the energy of the electron along the slowing down where the emission actually occurred, then the event is not physically valid; thus the CDF is 1 for such points.

As before, the above CDF is computed at the group edges and linearly interpolated to the energy of each electron. The piece-wise quadratic CDF is sampled with analytic inversion to produce the

energy of each emitted photon from an electron with initial energy E_e . The energy of the electron is not reduced after each sample because it has already been averaged into the definition of \bar{F} .

3 Angularly-dependent TTB Model

To improve the accuracy of the TTB model in MCNP, we have tested an angularly dependent thick-target bremsstrahlung model (ADTTB). This approach is similar to what is done in the ZADIG and DIANE code [3]. The primary difference in our method from the ZADIG model is we sample the scattering of the electron and photon emission energies based on continuous slowing down with Monte Carlo. The ZADIG version precomputes averaged outgoing photon tables based on infinite medium calculations based on an assumed flux shape within each energy groups; from the documentation is not clear if secondary electrons are included in these calculations. The ZADIG method also applies a weight correct to account for the transport of electrons based on the photon attenuation cross section. Our method comes at an increased computational cost, but is simple to implement in the existing MCNPv6.3 code base for testing and should improve correlations between the energy and direction of outgoing photons within a history.

In the ADTTB method, we perform a simplified version of the condensed history method used in the MCNP code [1]. In particular, we only model the scattering of electrons and the direction and energy distributions of emitted bremsstrahlung photons, both sampled along electron substeps. The displacement of electrons through different materials is neglected, removing the high cost of sampling straggling and tracking electrons through complicated geometries; this an acceptable assumption when interested in photon behavior through optically-thick media because photons have much longer mean-free-paths than electrons. This approach will correctly preserve the angular distribution of emitted photons from slowing electrons. This approach also neglects the effects of secondary electrons produced during slowing of the electron, e.g., knock-on electrons.

Following the condensed history algorithm, a fixed number of substeps are modeled per larger energy step. The range of each substep is chosen such that the total energy loss between energy steps is the difference between adjacent energy points in the grid. The algorithm for each electron created by an incident photon is summarized in the following listing:

1. For each electron energy step across energy group g
 - (a) For each substep $i = 1$ of N_{sub} substeps within energy step
 - i. Sample new direction of electron at end of substep from cumulative Goudsmit Saunderson (GS) scattering distribution [1].
 - ii. Compute energy step interpolation factor $f \in (0, 1)$ based on CSDA at random site within the substep as

$$f = \frac{E_g - E_{e,brem}}{E_g - E_{g+1}} \quad (5)$$

where E is a uniformly sampled energy within the current substep. Because energy is lost at a linear rate across step, this can be simplified to

$$f = (i - \eta)/(N_{sub}) \quad (6)$$

with a uniform random number η use to select within substep energy.

- iii. Sample an integer number of bremsstrahlung photons N_{brem} to be emitted over the substep from a Poisson distribution with mean

$$\bar{N}_{brem} = ((1 - f)\sigma_{brem,g} + f\sigma_{brem,g+1}) \frac{(R_{t,g} - R_{t,g+1})}{N_{sub}}. \quad (7)$$

- iv. If $N_{\text{brem}} > 0$, for this substep:
 - A. For each of N_{brem} photons to be emitted
 - Set photon emission energy to $E_{\gamma,\text{brem}} = \kappa E_{e,\text{brem}}$, where κ is sampled from the interpolated and tabulated quadratic CDF $F(\kappa, E_{e,\text{brem}})$.
 - Sample intermediate, independent electron direction from the GS CDF with a correction for the partial substep based on the chosen photon emission site within the substep. This is the same approach used in the condensed history algorithm.
 - Sample bremsstrahlung emission cosine relative to the intermediate electron direction using the bremsstrahlung tabular angle distribution
 - Isotropically sample bremsstrahlung emission azimuthal angle
 - Bank bremsstrahlung photon with sampled direction and energy for later transport

For the first group the electron traverses, it is necessary to adjust N_{sub} and f to account for the electron traversing only part of the group.

For this implementation, we have not implemented the case of biasing the number of emitted bremsstrahlung photons over each step or verified point-detectors in this implementation.

3.1 ADTTB Energy Sampling Simplification

The ADTTB algorithm includes additional simplifications in modeling bremsstrahlung energy losses, as compared to the condensed history algorithm. These simplifications were primarily added for ease of implementation because the goal of this work was only to prototype this approach. The additional simplifications listed here could be removed without much loss of performance to improve consistency with the condensed-history algorithm.

In the condensed history approach, the length of substeps, and thus the probability of sampling N_{brem} photons, is computed using the *total* range. However, the energy loss is treated differently for collisional (e.g., knock-on electrons) and radiative (i.e., bremsstrahlung emission) processes [1]. Electrons lose energy to collisional reactions through the continuous slowing down approximation based on the collisional stopping power, but energy loss due to bremsstrahlung is explicitly accounted for based on sampled bremsstrahlung photons along substeps. This primarily effects the electron energy at the emission site, which effects the distribution chosen for sampling κ and the outgoing photon energy. If multiple bremsstrahlung photons are emitted during the same substep, then the energy loss from the electron is taken into account for the emission of later photons. It is possible for electrons to transition to a new energy step after emitting a bremsstrahlung photon. The MCNP code manual [1] provides additional discussion about the treatment of energy losses for different events.

In the ADTTB approach, the probability of sampling N_{brem} photons is computed based on the total range and bremsstrahlung cross section the same as in the condensed history algorithm. However, both radiative and collisional energy losses and sampling are treated with the CSDA. Thus, we are only preserving the correct energy transferred to bremsstrahlung photons in expectation. It is possible for more energy than present in the initial electron's energy to be transferred to bremsstrahlung within an event; this is particularly likely when sampling multiple photons over a substep from the same κ distribution. This is also possible with the original TTB.

The bremsstrahlung energy distribution should be correct in expectation, similar to many other secondary particle approximations in MCNP, e.g., (n, γ) reactions. However, this is only true if the radiative processes range and bremsstrahlung cross sections are computed consistently, and is

subject to truncation error based on the linear interpolation of these properties based on electron energy. The results in the next section demonstrate that the range and cross sections are not sufficiently consistent to produce the same energy spectra within statistics.

4 Results

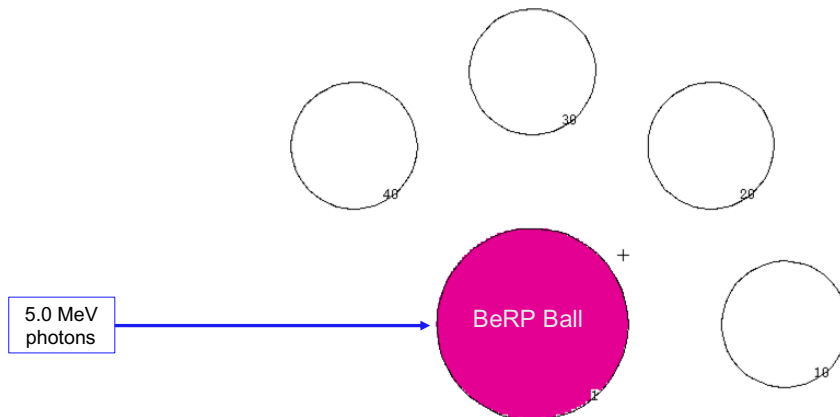


Figure 1: BeRP ball problem setup.

A simple incident photon source on the BeRP ball with photon tallies was modeled in the MCNP code, as depicted in Fig. 1. For the BeRP ball problem, a beam of photons at an energy of 5.0 MeV is monodirectionally incident on a ball of plutonium with radius 3.7938 cm. For this material, the range of a 5 MeV electron is 0.2 cm, so it is relatively thick to electrons. Spherical cells with a 2.5 cm radius are used for volumetric-flux photon tallies around the BeRP ball. The detectors are placed 10 cm from the center of the BeRP ball at angles of deflection from the incident beam of 0° , 45° , 90° , and 135° . The input files for electron transport and ADTTB method can be found in the appendix in Sec. B.1.1 and B.1.2, respectively. A DBCN option was added to turn on the ADTTB option for mode `p` problems. For this problem, the default energy cutoffs are such that for electron transport results the single-event and TTB models are not used.

Table 1 compares the photon volumetric flux tally results for the BeRP geometry using the condensed history electron transport (CH), TTB, and ADTTB methods, for each of the detectors surrounding the BeRP ball. Table 2 compares results for the different methods for `*F4` energy flux tallies. Also included in both tables is a row using CH with the `phys:e` card set to not produce electron-induced x-rays or knock-on electrons (labeled CH, no e^\pm secondaries); although electron-induced auger electrons are still present for this case, they are produced in negligible amounts compared to the primary electrons. From the electron balance tables of the CH results, only 0.006 electrons exit the BeRP sphere per incident photon.

Although this is a simple geometry with a relatively thick object, it demonstrates the deficiencies in the original TTB model. The TTB model has a much higher photon flux for the detector aligned along the beam, and only 11% of the transport energy flux at 90 degrees to the beam. The ADTTB method agrees with the transport results to within statistics along the beam, and has 10% disagreement in energy flux at 90 degrees. There was no observed difference in tally results between the CH and CH without secondary particles in the tallies.

Angle (deg)	0		45		90		135	
Method	ϕ (cm ⁻²)	ratio						
TTB	1.73e-04 ± 0.21%	1.43	9.32e-06 ± 0.78%	0.93	1.31e-06 ± 2.07%	0.19	1.98e-04 ± 0.17%	0.67
CH	1.21e-04 ± 0.24%	1.00	1.00e-05 ± 0.76%	1.00	6.96e-06 ± 0.90%	1.00	2.98e-04 ± 0.14%	1.00
ADTTB	1.20e-04 ± 0.24%	1.00	9.73e-06 ± 0.77%	0.97	6.37e-06 ± 0.94%	0.92	3.20e-04 ± 0.13%	1.07
CH, no e^\pm secondaries	1.21e-04 ± 0.24%	1.00	1.00e-05 ± 0.75%	1.00	6.95e-06 ± 0.90%	1.00	2.98e-04 ± 0.14%	1.00

Table 1: Comparison of flux tallies for BeRP ball problem.

Angle (deg)	0		45		90		135	
Method	$E\phi$ (MeV cm ⁻²)	ratio						
TTB	6.00e-04 ± 0.07%	1.14	1.28e-05 ± 0.27%	0.88	1.08e-06 ± 0.70%	0.11	9.18e-05 ± 0.06%	0.49
CH	5.25e-04 ± 0.25%	1.00	1.46e-05 ± 0.82%	1.00	9.49e-06 ± 1.00%	1.00	1.86e-04 ± 0.17%	1.00
ADTTB	5.27e-04 ± 0.08%	1.00	1.42e-05 ± 0.26%	0.97	8.51e-06 ± 0.33%	0.90	1.88e-04 ± 0.05%	1.01
CH, no e^\pm secondaries	5.25e-04 ± 0.25%	1.00	1.46e-05 ± 0.81%	1.00	9.51e-06 ± 1.00%	1.00	1.86e-04 ± 0.17%	1.00

Table 2: Comparison of energy-weighted flux tallies for BeRP ball problem.

To investigate the difference between the solutions, we have used the PTRAC output from the MCNP code to histogram the initial energy, spatial, and angle distribution of all bremsstrahlung photons produced within the BeRP ball with 10^6 histories. Figure 2 compares normalized probability densities of bremsstrahlung photons for cosine with respect to the beam axis (i.e., the x-axis) and cosine with respect to the perpendicular axis to the beam (i.e, the y-axis); the relative deviation compared to the condensed-history solution is given for each as well. The angular distributions show very good agreement between the transport solutions and the ADTTB method, whereas the TTB method is artificially forward peaked.

Figure 3 compares the *normalized* spatial density of photon emission sites along the x axis. At the front of the sphere, the ADTTB method is artificially higher than the transport solutions because of the lack of spatial displacement of electrons. The difference in photon attenuation based on the emission location of bremsstrahlung photons near the front of the sphere likely contributes to the discrepancy between the ADTTB method and transport for the 90 degree tally, for this simplified problem. The TTB method is more spatially distributed through the sphere because of the forward peaking of emitted photons, which ultimately produce secondary electrons and bremsstrahlung photons.

Method	$N_{\text{brem}} / \text{history}$	$E_{\text{brem,tot}} / \text{history}$
TTB	7.85	7.6439E-01
CH	8.49	7.6963E-01
ADTTB	7.69	7.2909E-01
CH, no e^\pm secondaries	7.50	7.5189E-01

Table 3: Comparison of average number of bremsstrahlung photons and total energy from bremsstrahlung produced per history, for each method.

Table 3 details the average number of bremsstrahlung photons produced and total energy from all bremsstrahlung photons produced, per starting source particle, for each of the simulations. Figure 4 compares the energy distribution of bremsstrahlung photon tracks and Figure 5 compares the energy distribution of all photons within the sphere. The bremsstrahlung distribution is computed from the PTRAC file, whereas the total spectrum is tallied using a volumetric flux tally within the sphere with all bins less than 0.1% error.

The total number of bremsstrahlung photons produced for the TTB and ADTTB models disagree. Although they are using the same data and should agree on average, the difference in number is a result of the energy spectra of outgoing photons and the cutoff energy of 1 keV for this problem. For a given incident electron energy, the ADTTB and TTB model are sampling the same total number of photons on average, but the ADTTB is more likely to sample bremsstrahlung photons below the energy cutoff. This is because the TTB method is sampling from an approximate distribution for κ , and then multiplying by the initial energy of the electron produced for all emitted photons. However, the ADTTB method is sampling from a distribution of κ for the electron energy at the emission point along the slowing path of the electron. The energy spectra for TTB is harder than the transport results as well.

The CH results produce more energy and photons from bremsstrahlung. This is primarily the result of secondary electrons. The results for CH without secondary electron x-rays and knock-on electrons produce bremsstrahlung photon energy closer to the ADTTB method.

Compared to the transport results, the ADTTB method is producing generally a lower energy spectrum of bremsstrahlung photons. The cause of this is believed to be due to the ADTTB method using the CSDA to determine the energy of the electron at bremsstrahlung emission sites rather than explicitly sampling radiative energy loss, as discussed in Sec. 3.1. Although not shown here, the softer energy spectrum was also observed in infinite medium result using the BeRP material. However, for an infinite medium of water, all methods agreed more consistently on the number and energy of emitted bremsstrahlung photons.

4.1 Performance Comparisons

Method	Relative Speedup
TTB	502.6
CH	1.0
ADTTB	19.6
CH, no e^\pm secondaries	6.0

Table 4: Comparison of computational performance for the BeRP ball problem.

Table 4 demonstrates the relative speed for each of the models. The ADTTB model is significantly slower than the original TTB model, but still faster than the full electron transport approach by a factor of 20. This problem provides a worse-case scenario for efficiency of the ADTTB model because there is almost no cost to tracking the electron in the simple geometry for the full transport approach. Using a profiler, for the berp ball problem, about 90% of the modified TTB total run time is spent in the TTB routine, with 80% of the total runtime spent in the `escat` routine, which is responsible for scattering the electrons. Because scattering is formulated over electron substeps, there are many samples for each generated electron (13 for plutonium), linear in cost with the log-

arithm of the energy of the initial electron. Inverting the GS distribution, which requires a search through the CDF is the dominant source of the computational cost. Using the alias sampling method may improve the efficiency of this portion of the code modestly.

Method	Relative Speedup
TTB	17.9
CH	1.0
ADTTB	14.8

Table 5: Comparison of computational performance for the Zubal phantom problem.

The modified Zubal phantom problem from a MCATK radiography test was also simulated with the MCNP code for each of the methods. This problem consisted of a 10 MeV disk beam of photons incident on a phantom head containing 13 materials and a complicated lattice geometry that has been used to generate LNK3DNT problems in the MCATK python examples directory; no tally results were measured as we were just interested in performance.

The results for the Zubal phantom are given in Table 5. In this case, the ADTTB method is only 22% slower than the original TTB method, but still 15 times faster than the condensed history approach. The Zubal phantom problem represents more realistic computational memory patterns than the BeRP ball as tracking is more expensive, the memory footprint is larger, there are more materials, and adjacent cells require different data. These additional costs make the arithmetic costs of sampling the GS distribution less significant, as expected in most large Monte Carlo simulations.

Using less substeps per energy step would obviously also improve performance. However, the number of substeps per energy step was chosen per material primarily to optimize the distribution of secondary particles[4, 1], so it may not be possible to reduce this number much and preserve angular accuracy. One option to improve performance potentially is below some energy threshold, sample the total number of emitted photons over the remaining steps as in the original TTB model; then if the sampled number is zero, don't model the electron scattering.

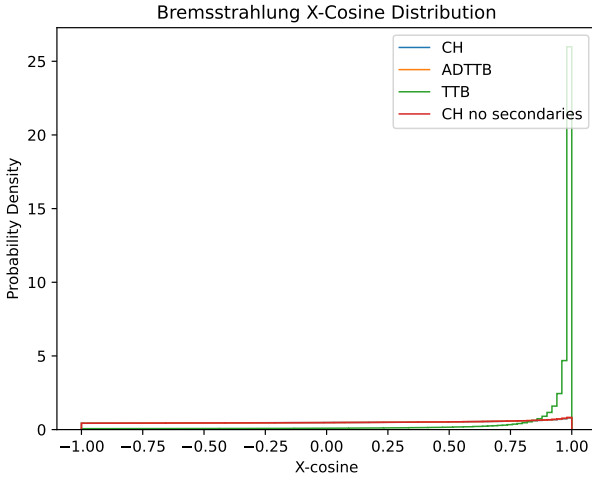
5 Future Work

The ADTTB method was found to be a significant improvement over the original TTB method for photon problems with higher energy and a strong angular dependence. This model should be tested on problems with more material variation and slightly thinner materials. We should implement the explicit sampling of bremsstrahlung energy loss for the ADTTB method to confirm that the difference in energy spectra is from using the continuous slowing down approximation for both collisional and radiative losses. As the ADTTB method is relatively expensive, it may be of interest to compare to a method of TTB where we simply tally the outgoing angle-energy distribution of bremsstrahlung photons from infinite medium calculations, and then sample it for each generated electron, as in Ref. [3]. While pre-computing the data would be more expensive and introduce some truncation error, it could be reused for multiple simulations with the same materials present and would capture the effect of secondary electrons.

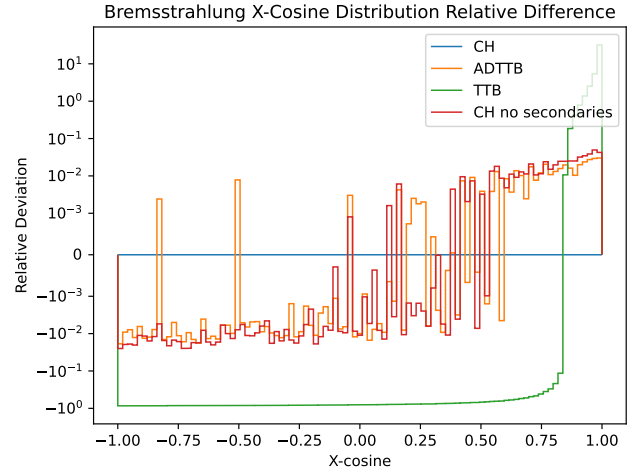
In future work, to improve on the ADTTB method, as the GS distribution is accurate for any substep length, we should investigate the possibility of using less substeps per energy step; it may be possible to preserve accuracy of bremsstrahlung photons compared to other secondary processes

because the bremsstrahlung angular distribution may provide some additional smoothing. This method could also be applied to radiography simulations where the same strong directionality of photons is relevant, but point-detectors are used.

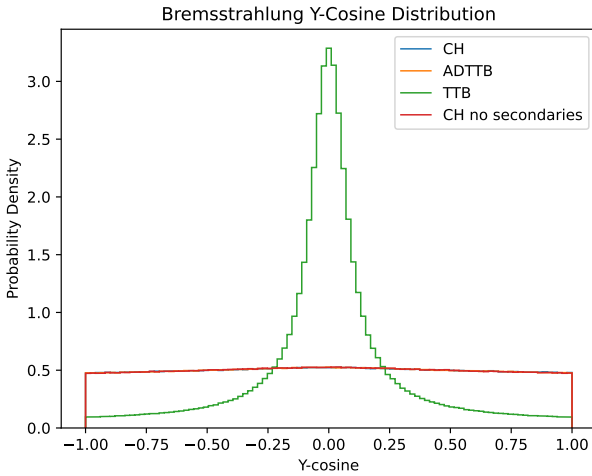
Although not strictly related to this work, we should also investigate using the semi-analytic fits used by PENELOPE [2] for sampling and point-detector computations of bremsstrahlung photon emission. Currently, MCNP samples a complex tabular distribution during transport and then uses an approximate distribution for point-detector contributions. The semi-analytic fits from PENELOPE should be more accurate because they are based on newer models, but they also should be sufficiently simple to compute the point-detector contributions.



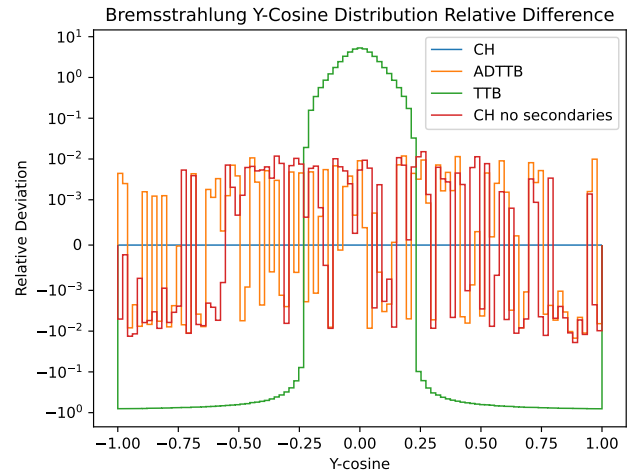
(a) x -cosine probability density.



(b) x -cosine probability density deviation.

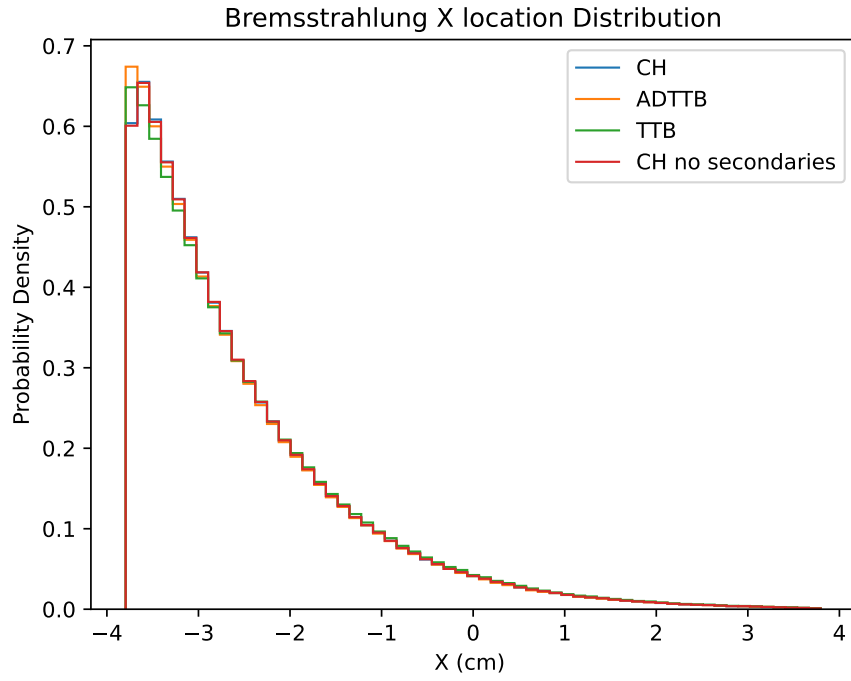


(c) y -cosine probability density.

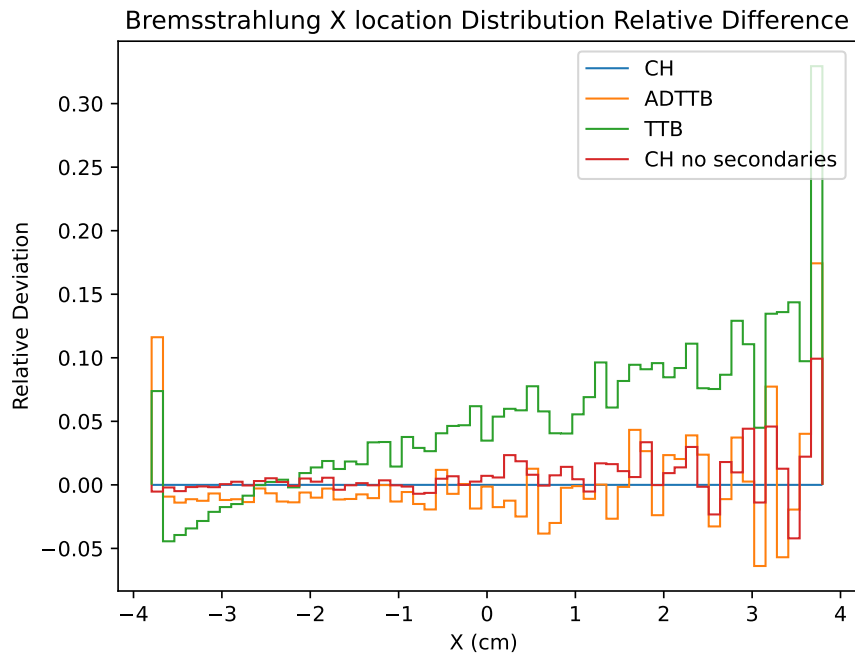


(d) y -cosine probability density deviation.

Figure 2: Comparison of angular distributions for emitted bremsstrahlung photon tracks with different methods. Deviations are the relative difference w.r.t. to condensed history results, plotted on a logarithmic scale.

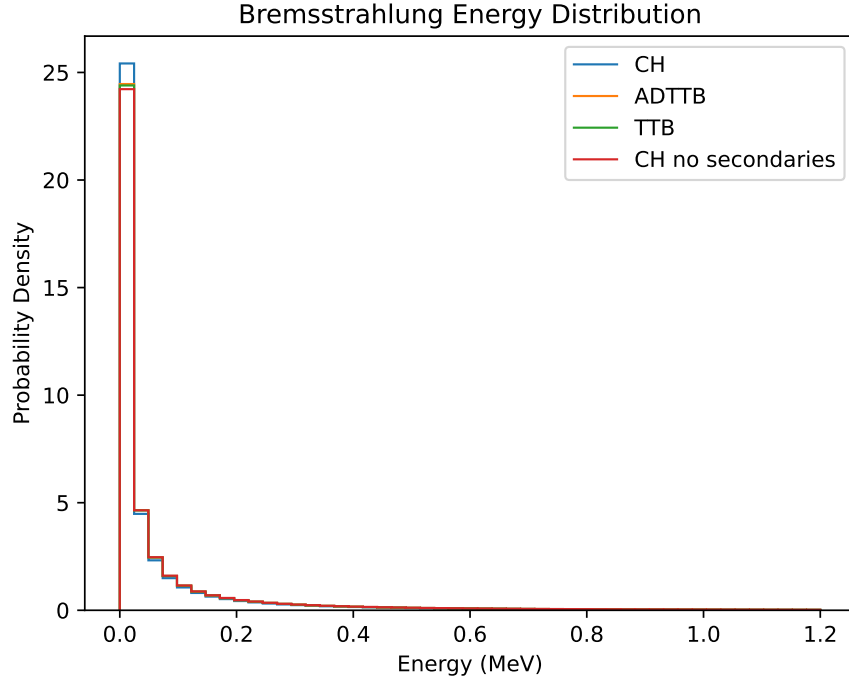


(a) Probability density of emission location x coordinate.

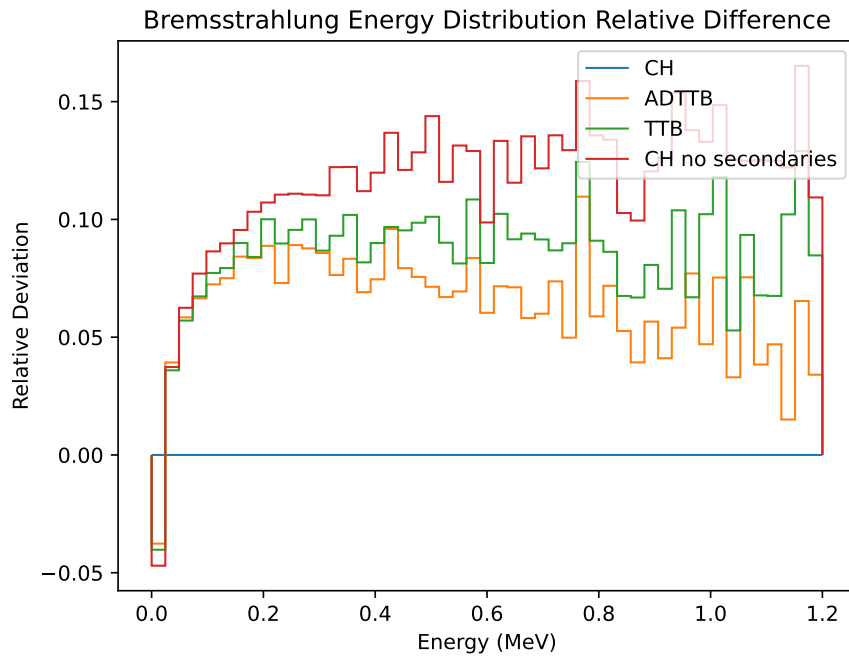


(b) Relative error in probability density.

Figure 3: Comparison of bremsstrahlung photon track emission location x coordinate (along the beam) within the sphere.



(a) Energy spectrum probability densities.



(b) Probability density relative errors.

Figure 4: Comparison of bremsstrahlung photon energy spectra within the BeRP ball. Note that the bremsstrahlung distribution is normalized over bremsstrahlung photon tracks created, not per history.

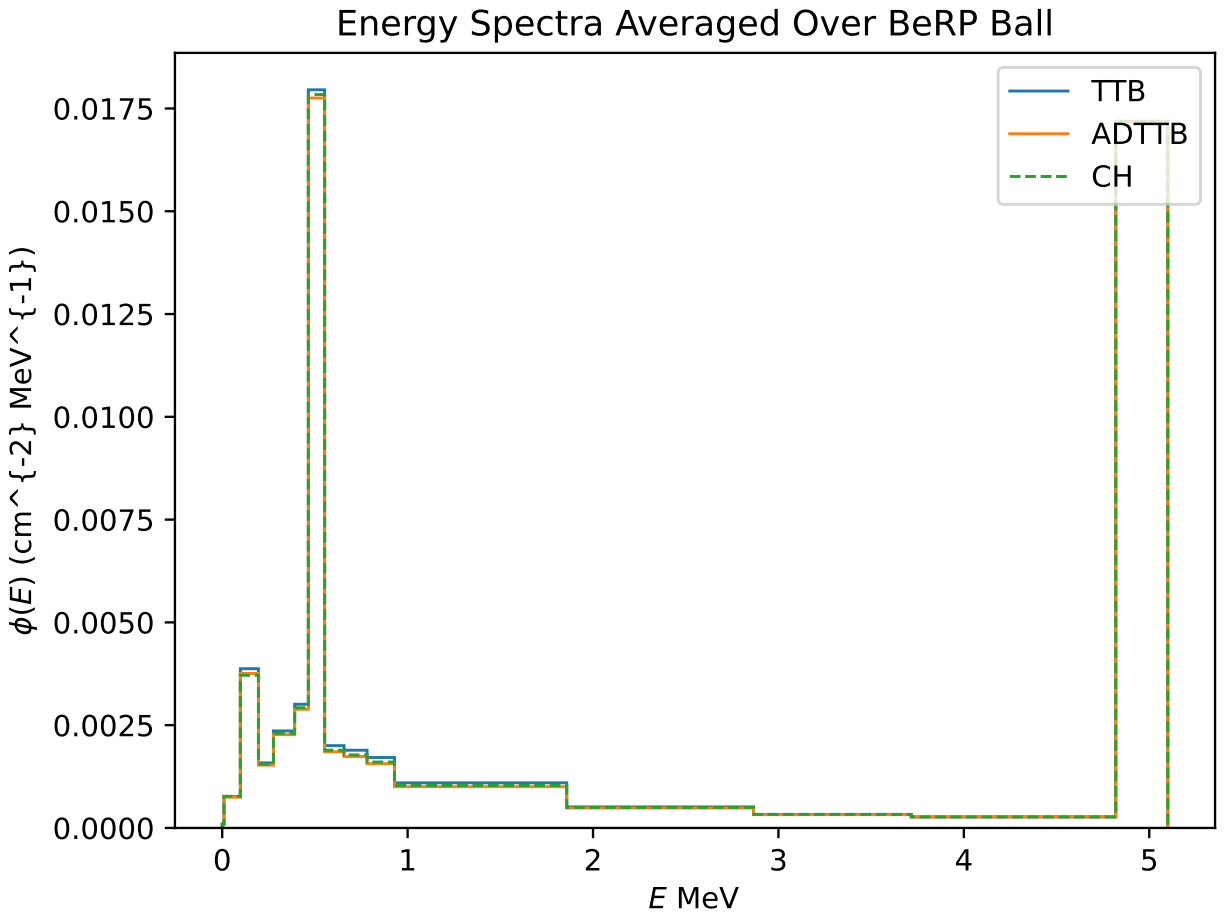


Figure 5: Comparison of total photon energy spectra within the BeRP ball. Note that the total energy distribution is a measured photon flux per history.

References

- [1] J. A. Kulesza *et al.*, “MCNP[®] Code Version 6.3.0 Theory & User Manual,” Los Alamos National Laboratory, Los Alamos, NM, USA, Tech. Rep. LA-UR-22-30006, Rev. 1, September 2022. [Online]. Available: <https://www.osti.gov/biblio/1889957>
- [2] F. Salvat, J. M. Fernández-Varea, J. Sempau *et al.*, “Penelope-2011: A code system for monte carlo simulation of electron and photon transport,” in *Workshop Proceedings, Barcelona, Spain*, vol. 5, 2011.
- [3] S. Menard, “Zadig: Latest improvements to bremsstrahlung treatment and in-flight annihilation scheme,” CEA, Tech. Rep., 2006.
- [4] T. M. Jenkins and W. R. Nelson, Eds., *Monte Carlo Transport of Electrons and Photons*. Springer, 1988.
- [5] G. Rybicki and A. Lightman, *Radiative Processes in Astrophysics*, ser. Physics textbook. Wiley, 2004, pp. 109–110.

A Discussion of MCNP Electron Transport Implementation Details and Potential Improvements

The following is a list of observations and derivations related to the treatment of condensed-history electron scattering and bremsstrahlung models in MCNP6, version 6.3. Most of the models in MCNP are originally from the ITS3 code, but documentation of many of the approximations and derivations for equations used by the code are difficult to find in references and opaque to developers who are not electron transport experts. Thus, we have noted some of the oddities and derivations that we have come across within the code for future reference to MCATK and MCNP developers. Where appropriate, these details will be added to the latest MCNP manual. We have also noted a couple observations of places where the algorithm could potentially be improved.

- For sampling of number of bremsstrahlung photons, MCNP samples from a Poisson distribution in condensed history, but samples from a uniform integer number for the TTB model and older ITS models. Over a substep of length D , the probability of producing any photons is given as $1 - \exp(-D\sigma)$. Thus, we can throw a random number, and check if $\eta \leq 1 - \exp(-D\sigma)$, then photons are produced. Using a first order Taylor series, we can expand the exponent, so the process is to check if $\eta \leq 1 - \exp(-D\sigma) \approx 1 - (1 - D\sigma) = D\sigma$. This gives us the usual integer truncation of a random sampled number of $N = \lfloor \eta + D\sigma \rfloor$ used in the TTB model.
- MCNP provides a simple bremsstrahlung angular emission model that is used for point detectors and optionally used for consistent sampling of emission photons. The origin of this model is not explicitly stated in the manual or reference collection currently. It can be derived by assuming that emitted bremsstrahlung photons are isotropic in the frame of the electron, i.e., a frame moving in the same direction as the electron but where the electron is at rest. The cosine of the emitted photon with respect to the electron in this frame μ' is related to the cosine of the emitted photon in the lab frame through the following Lorentz transformation (Penelope Manual, 2011, Section 3.3):

$$\mu = \frac{\mu' + \beta}{1 + \beta\mu'}, \quad (8)$$

where β is the ratio of the velocity of the electron to the speed of light. This transformation is referred to as the aberration of light in astrophysics text books, e.g., Ref. [5]. Transforming the isotropic distribution $p'(\mu) = 1/2$, $\mu \in [-1, 1]$ to the lab frame gives

$$p(\mu) = p(\mu') \frac{d\mu}{d\mu'} = \frac{1 - \beta^2}{2(1 - \beta\mu)^2}. \quad (9)$$

This is the simple probability distribution that MCNP uses and is the high-energy limit as $\beta \rightarrow 1$.

- We should consider alternative forms of bremsstrahlung cross section formulation for the simplified bremsstrahlung model used for point detector contribution. In particular, PENELOPE has an analytic form (equation 3.171 in the 2011 manual) that could be used, if the data is readily available. It would be efficient to evaluate and is much closer to the true distribution. Alternatively, we may be able to invert the tables used by MCNP at an increased expense.
- The angular sampling of emitted bremsstrahlung photons in brems.F90, which was used for the angularly-dependent TTB implementation, can be a bit confusing at first. Bremsstrahlung

photons are sampled relative to the electron direction from somewhere along a substep. However, MCNP samples the angular deflection of an electron over the entire substep using the `escat` routine based on a tabulated form of the GS distribution. However, that samples a direction of the electron over multiple scatters at the end of the substep. Since the bremsstrahlung photon is emitted somewhere along the substep, it is based on the direction of the electron after less deflections. How MCNP implements this is to sample a direction of the electron again, and apply a correction (explained in next bullet) to account for the fact the electron has gone less than a full substep, even though the data we have is for the entire substep length. From the direction of that intermediate electron, the bremsstrahlung angular distributions are sampled. This results in two azimuthal direction samplings (calls to `rotas`): one for the partial step electron using the sampled scatter cosine, and then a second using the sampled bremsstrahlung photon emission cosine. The original electron path is not adjusted in anyway when a bremsstrahlung photon is emitted, because this is consistent with the multiple scattering theory of electrons. One odd side effect of this is that the bremsstrahlung direction (particularly the azimuthal angle), can be very different from the actual electron path. This seems like an unnecessary introduction of only preserving the mean behavior.

- The condensed history algorithm depends on tabulated CDFs for the GS distribution that is precomputed based on a particular substep size for each material and energy group. The algorithm then uses a modification to the sampled deflection for partial substeps in the `escat` routine. I have not found the original derivation of this relation, so I have attempted to derive it along the following lines: based on the GS theory, the distribution of scattering cosines μ is defined, for a particular energy, as

$$p(\mu, s) = \sum_{l=0}^{\infty} \left(l + \frac{1}{2} \right) \exp(-sG_l) P_l(\mu) \quad (10)$$

where s is the substep pathlength, $P_l(\mu)$ is the l -th Legendre polynomial, and

$$G_l = 2\pi \frac{N_a}{A} \int_{-1}^1 [1 - P_l(\mu)] \sigma(\mu) d\mu \quad (11)$$

is the l -th coefficient found from taking a moment of the differential cross section with the above weighting; here N_a is Avogadro's number and A is the atomic weight. Note that G_l is not a function of s . The mean value of the deflection cosine μ can be found by integrating the above formula weighted against $P_1(\mu)$ and using orthogonality to get $\bar{\mu} = \exp(-G_1 s)$. Then, we can do a Taylor expansion of $1 - \bar{\mu}$ ($\bar{\mu} \approx 1$ for small s):

$$1 - \bar{\mu} = 1 - \exp(-G_1 s) \approx 1 - (1 - G_1 s) = G_1 s \quad (12)$$

Since G_1 is a constant with respect to s and $\bar{\mu}$, for a given energy and material, we can take a ratio of this expression for a pathlength s' less than s (both small), and solve for μ' to get:

$$\mu' = 1 - (1 - \mu) \frac{s'}{s}. \quad (13)$$

This is the correction used by the `escat` routine to sample deflection cosines for pathlengths that are less than the substep length. Intuitively, this is also just a linear interpolation of the sampled μ w.r.t. s because $\mu = 1$ for $s = 0$. Potentially this could be improved by doing a second-order expansion of μ , but because s is generally small, it may not provide much improvement. It would be an interesting exercise to change the substep sizes in MCNP and recompute the true distributions and compare to this approximation for different values.

- The way that MCNP computes the differential scattering cross section used for evaluation of the GS distribution is obtuse code. There is a reference in one of the comments to an older paper that explains the original derivation. Newer evaluations are available that are used by PENELOPE in an ASCII database are available here <https://www.icru.org/report/elastic-scattering-of-electrons-and-positrons-icru-report-77/>, which would be relatively straightforward to integrate. This is also used by GEANT4 for its GS distribution. It is noted that PENELOPE and GEANT4 provide alternative models that don't require such a small, fixed substep size, by sampling a mix of "soft" and "hard" scatters.
- The MCNP implementation using data from the el03 library (ITS3 or later) allows for 1 or more photons per substep to be emitted, based on a Poisson process distribution. The implementation in `brems` is not obvious because it mixes a loop and `gotos`. The loop is based on biasing, and for unbiased problems only has one iteration per history. However, a `goto` is used to sample the Poisson distribution that returns to the start of the loop if multiple photons need to be emitted.
- The current TTB implementation (in `ttbr.F90`) appears to be suboptimal for mixed materials. In particular, it just sets `mkc=mat(pbl%i%icl)`, which ultimately is using the material that the electron-creating photon reaction sampled. A dominant material treatment is probably more optimal. This is probably incorrect for LNK3DNT problems. This issue has already been created and reported under the MCNP issue tracker.

B Input Files

B.1 BeRP Ball Problem Input Decks

The TTB bremsstrahlung input will use the ADTTB method if using the `prototype/angular_ttb_squashed` branch of the MCNP git repository.

B.1.1 Electron Transport Input

```
Photon beam with energy 4 MeV hits burpball includes e
c ccccccccccccccccccccccccccccccccccccccccccccccccccccccccccccccccccccccccc c
c                                                                                   c
c                               Cell Cards                                         c
c                                                                                   c
c ccccccccccccccccccccccccccccccccccccccccccccccccccccccccccccccccccccccccc c
10 100 -19.85 -1                               imp:p,e=1
20 0      -2                               imp:p,e=1
30 0      -3                               imp:p,e=1
40 0      -4                               imp:p,e=1
50 0      -5                               imp:p,e=1
60 0      -6                               imp:p,e=1
70 0      -7                               imp:p,e=1
80 0      -8                               imp:p,e=1
90 0          #10 #20 #30 #40 #50 #60 #70 #80 -23  imp:p,e=1
99 0          +23                               imp:p,e=0

c ccccccccccccccccccccccccccccccccccccccccccccccccccccccccccccccccccccccccc c
```



```

c ccccccccccccccccccccccccccccccccccccccccccccccccccccccccccccccccccccccccc c
c -----Surface tally on BERP Ball only looking at electrons----- c
c ccccccccccccccccccccccccccccccccccccccccccccccccccccccccccccccccccccccccc c
*f101:e 1 $ tally on surface of BURP
f111:e 1 $ tally on surface of BURP
e101 9.4129E-03 9.7656E-02 1.9531E-01 2.7621E-01 3.9062E-01
      4.6453E-01 5.5243E-01 6.5695E-01 7.8125E-01 9.2907E-01
      1.8581 2.8656 3.7163 4.8194
e111 9.4129E-03 9.7656E-02 1.9531E-01 2.7621E-01 3.9062E-01
      4.6453E-01 5.5243E-01 6.5695E-01 7.8125E-01 9.2907E-01
      1.8581 2.8656 3.7163 4.8194
c ccccccccccccccccccccccccccccccccccccccccccccccccccccccccccccccccccccccccc c
c ----Surface flux tally on BERP Ball only looking at electrons---- c
c ccccccccccccccccccccccccccccccccccccccccccccccccccccccccccccccccccccccccc c
*f102:e 1 $ tally on surface of BURP
f112:e 1 $ tally on surface of BURP
e102 9.4129E-03 9.7656E-02 1.9531E-01 2.7621E-01 3.9062E-01
      4.6453E-01 5.5243E-01 6.5695E-01 7.8125E-01 9.2907E-01
      1.8581 2.8656 3.7163 4.8194
e112 9.4129E-03 9.7656E-02 1.9531E-01 2.7621E-01 3.9062E-01
      4.6453E-01 5.5243E-01 6.5695E-01 7.8125E-01 9.2907E-01
      1.8581 2.8656 3.7163 4.8194
c ccccccccccccccccccccccccccccccccccccccccccccccccccccccccccccccccccccccccc c
c -----Surface tally on BERP Ball only looking at photon----- c
c ccccccccccccccccccccccccccccccccccccccccccccccccccccccccccccccccccccccccc c
*f121:p 1 $ tally on surface of BURP
f131:p 1 $ tally on surface of BURP
e121 9.4129E-03 9.7656E-02 1.9531E-01 2.7621E-01 3.9062E-01
      4.6453E-01 5.5243E-01 6.5695E-01 7.8125E-01 9.2907E-01
      1.8581 2.8656 3.7163 4.8194
e131 9.4129E-03 9.7656E-02 1.9531E-01 2.7621E-01 3.9062E-01
      4.6453E-01 5.5243E-01 6.5695E-01 7.8125E-01 9.2907E-01
      1.8581 2.8656 3.7163 4.8194
c ccccccccccccccccccccccccccccccccccccccccccccccccccccccccccccccccccccccccc c
c ----Surface flux tally on BERP Ball only looking at photon----- c
c ccccccccccccccccccccccccccccccccccccccccccccccccccccccccccccccccccccccccc c
*f122:p 1 $ tally on surface of BURP
f132:p 1 $ tally on surface of BURP
e122 9.4129E-03 9.7656E-02 1.9531E-01 2.7621E-01 3.9062E-01
      4.6453E-01 5.5243E-01 6.5695E-01 7.8125E-01 9.2907E-01
      1.8581 2.8656 3.7163 4.8194
e132 9.4129E-03 9.7656E-02 1.9531E-01 2.7621E-01 3.9062E-01
      4.6453E-01 5.5243E-01 6.5695E-01 7.8125E-01 9.2907E-01
      1.8581 2.8656 3.7163 4.8194
c ccccccccccccccccccccccccccccccccccccccccccccccccccccccccccccccccccccccccc c
c ccccccccccccccccccccccccccccccccccccccccccccccccccccccccccccccccccccccccc c
c
print

```

B.1.2 Angularly-Dependent Thick-Target Bremsstrahlung Input

Photon beam with energy 5 MeV hits burpball

```
c ccccccccccccccccccccccccccccccccccccccccccccccccccccccccccccc c
c
c                               Cell Cards                               c
c
c
c ccccccccccccccccccccccccccccccccccccccccccccccccccccccccccccc c
1  100 -19.985  -1          imp:p=1 $ berp
2   0   -10          imp:p=1 $ east detector
3   0   -20          imp:p=1 $ NE detector
4   0   -30          imp:p=1 $ N detector
5   0   -40          imp:p=1 $ NW detector
6   0   (10 20 30 40) (1) -99 imp:p=1 $ air around detectors and slab
99  0    99          imp:p=0 $ kill zone
```

```
c ccccccccccccccccccccccccccccccccccccccccccccccccccccccccccccc c
c
c                               Surface Cards                             c
c
c ccccccccccccccccccccccccccccccccccccccccccccccccccccccccccccc c
1  so  3.7938          $ BERP Sphere
10 sph  10  0  0 2.5          $ E Detector
20 sph  7.071068 7.071068 0 2.5 $ NE Detector
30 sph  0  10  0 2.5          $ N Detector
40 sph -7.071068 7.071068 0 2.5 $ NW Detector
99 so  1000.0          $ Outer universe
```

```
c ccccccccccccccccccccccccccccccccccccccccccccccccccccccccccccc c
c
c                               Data Cards                               c
c
c ccccccccccccccccccccccccccccccccccccccccccccccccccccccccccccc c
```

```
mode p
nps 1e9
rand gen=2
```

```
c ccccccccccccccccccccccccccccccccccccccccccccccccccccccccccccc c
c -----Material Specifications----- c
c ccccccccccccccccccccccccccccccccccccccccccccccccccccccccccccc c
m100 94238 0.00020
      94239 0.93730
      94240 0.05960
      94241 0.00268
      94242 0.00028
```

```
c ccccccccccccccccccccccccccccccccccccccccccccccccccccccccccccc c
c -----Source Specifications----- c
c ccccccccccccccccccccccccccccccccccccccccccccccccccccccccccccc c
```

```

sdef par=p pos= -20 0 0 erg=5.0 vec= 1 0 0 dir= 1
c ccccccccccccccccccccccccccccccccccccccccccccccccccccccccccccccccc c
c -----fmesh surrounding the detectors and BURP ball----- c
c ccccccccccccccccccccccccccccccccccccccccccccccccccccccccccccccccc c
c fmesh4:p GEOM= xyz ORIGIN= -11.0 -11.0 -11.0
c IMESH= 11.0 IINTS= 100
c JMESH= 11.0 JINTS= 100
c KMESH= 11.0 KINTS= 100
c ccccccccccccccccccccccccccccccccccccccccccccccccccccccccccccccccc c
c -----Flux tally for detectors only looking at photons----- c
c ccccccccccccccccccccccccccccccccccccccccccccccccccccccccccccccccc c
c fc4 flux tally
f24:p 2
fc24 Flux Tally at (0.0,10.0,0.0 r=2.5)
f34:p 3
fc34 Flux Tally at (sqrt(50),sqrt(50),0.0 r=2.5)
f44:p 4
fc44 Flux Tally at (0.0,10.0,0.0 r=2.5)
f54:p 5
fc54 Flux Tally at (-sqrt(50),sqrt(50),0.0 r=2.5)
*f124:p 2
fc124 Energy Tally at (0.0,10.0,0.0 r=2.5)
*f134:p 3
fc134 Energy Tally at (sqrt(50),sqrt(50),0.0 r=2.5)
*f144:p 4
fc144 Energy Tally at (0.0,10.0,0.0 r=2.5)
*f154:p 5
fc154 Energy Tally at (-sqrt(50),sqrt(50),0.0 r=2.5)
f4:p 1
fc4 Flux tally over berp ball
*f14:p 1
fc14 Energy-flux tally over berp ball
c ccccccccccccccccccccccccccccccccccccccccccccccccccccccccccccccccc c
c -----Surface tally for photons leaving the ball
c ccccccccccccccccccccccccccccccccccccccccccccccccccccccccccccccccc c
f101:p 1 $ energy tally on right side of slab
fc101 Tally number of photons leaving the right side of slab
*f111:p 1 $ tally on surface of BURP
fc111 Tally photon energy leaving right side of the slab
e0 9.4129E-03 9.7656E-02 1.9531E-01 2.7621E-01 3.9062E-01
4.6453E-01 5.5243E-01 6.5695E-01 7.8125E-01 9.2907E-01
1.8581 2.8656 3.7163 4.8194 5.100
dbcn 6j 1 $ DBCN option added in ADTTB branch to turn on modified TTB, otherwise regular TTB
cut:e j 1.0E-06
print
prdmp 2j -1

```